

Dear Florent, dear Reviewers,

besides the changes which are already indicated in the response letters in the TCD comments section, additional changes in the manuscript were necessary to comply with all your comments during the first revision. Overall, these changes greatly helped to improve the manuscript, this is at least what I think. In particular:

- We have discarded the explicit emphasis on crystal habit in the title and throughout the paper and replaced it by a more general emphasis of “morphology”. This allows to discuss all quantities (SSA, crystal habit, Euler characteristic) as different aspects of morphology. As a consequence, we have combined our results on crystal habit and Euler characteristic in one part in the results subsection “Influence of other morphological properties”. Therefore we moved our results on the Euler characteristic, which were before previously simply dumped in the “overview” section, to this new section. This also helped to clarify the confusion about the influence of stress on the SSA evolution (raised by Reviewer 1)
- As a consequence of these strategic changes, the introduction and discussion were significantly rewritten to allow for a concise presentation. This also helped to better explain the main goal of the present paper, which was criticized by Reviewer 2.
- By request from the Editor, we have included a comparison of the present parametrization to an existing one, which now appears as the last section in the results part.

A final comment/request: We know that the community has recently decided to consistently provide SSA values in units of m^2/kg . This paper is however the last of a sequence of related papers about new snow (Schleef and Löwe 2013, Schleef et al 2014a, Schleef et al 2014b) where the SSA was always given in units of $1/\text{mm}$ (to stress its meaning of an inverse length scale). For consistency between within these related results, we thus decided to stick to $1/\text{mm}$ also in this paper for a last time. The conversion between both is given in the methods section anyway.

All changes made to the document are monitored by a latex-diff which is attached to this letter.

Kind regards,
Henning Löwe

Influence of stress, temperature and crystal **habit morphology** on isothermal densification and specific surface area decrease of new snow

S. Schlee, H. Löwe, and M. Schneebeli

WSL Institute for Snow and Avalanche Research SLF, Davos, Switzerland

Correspondence to: Henning Löwe
(loewe@slf.ch)

Abstract. Laboratory-based, experimental data for the microstructural evolution of new snow is scarce, though applications would benefit from a quantitative characterization of the main **mechanism underlying the initial microstructural changes** influences. To this end we have analyzed the metamorphism and concurrent densification of new snow under isothermal conditions by means of X-ray microtomography and compiled a comprehensive data set of 45 time series **covering the practically relevant short time behavior within the first**. **In contrast to previous measurements on isothermal metamorphism on time scales of weeks to months, we analyzed the initial** 24-48 h **in-of snow evolution at high temporal resolution of three hours**. The data set **comprises** ~~comprised~~ natural and laboratory grown snow and experimental conditions **include** ~~included~~ systematic variations of overburden stress, temperature and crystal habit to address the main influences on specific surface area (SSA) decrease rate and densification rate in a **natural** snowpack. For all conditions we **find a linear increase of the density with the** **found a linear relation between density and** SSA, indicating that metamorphism has **a key-an immediate** influence for the densification of new snow. **Corroborated by the analysis of the individual influences of external conditions we** **The slope of the linear relation however depends on the other parameters which were analyzed individually to** derive a best-fit parametrization for the SSA decrease rate and the densification rate **as required for applications**. **In the investigated parameter range, we found that the initial value of the SSA constituted the main morphological influence on the SSA decrease rate. In turn, the SSA decrease rate constituted the main influence on the densification rate.**

20 1 Introduction

The temporal evolution of new snow is delicate, since fast changes of bulk density or specific surface area (SSA) as key microstructural characteristics occur ~~shortly~~ within hours after snowfall. Various applications rely on a quantitative understanding of these initial snowpack processes. For avalanche prediction a fast or slowly densifying snowpack eventually discerns between conditions of high or low snowpack stability ~~and initial~~. Initial modeling uncertainties of the densification ~~density~~ will propagate and persist through the entire season (Steinkogler et al., 2009). The density of snow is also important for hydrological applications where estimates of snow water equivalent are commonly obtained from snow height measurements of meteorological stations via empirical correlations between height and density. The development of these parametrizations is complicated by intermediate snow falls and ~~its short time evolution during subsequent~~ short time densification (McCreight and Small, 2013). If the state of the snowpack is instead monitored via remote sensing, the key quantity is snow albedo which is mainly determined via SSA (Flanner and Zender, 2006) ~~and even~~. Even thin layers of new snow have a measurable impact on the total snow albedo (Perovich, 2007). Finally, the validation of winter precipitation schemes for meteorological models also rely on the connection between airborne crystal sizes (which might be related to the inverse SSA) and the bulk densities of new snow (Thompson et al., 2008).

~~From a modeling perspective~~ For many applications ground-truth measurements are not available and the evolution of new snow on the ground ~~can~~ must be addressed by snowpack ~~models which modeling~~. Snowpack models primarily aim at a description of densification rates in terms of overburden and temperature (Jordan, 1991; Lehning et al., 2002; Vionnet et al., 2012). ~~Some of these~~ To cope with the needs of applications for metrics of crystal size and morphology, some of the models also include ~~the microstructure in terms of empirical~~ empirical, microstructural parameters such as grain size, dendricity ~~and sphericity~~. ~~These~~, sphericity or coordination number. The choice of these microstructural parameters is motivated by the natural variations of snow crystal habits plus some metric of connectivity. These empirical parameters are however ambiguous ~~to be determined objectively and~~ and cannot be measured objectively for aggregated snow. Therefore recent versions of snowpack models ~~aim at replacing~~ have replaced the empirical parameters by objective ones which can be uniquely defined for arbitrary bicontinuous structures. Of primary interest was the replacement of grain size by the ~~optical radius (or inverse specific surface area)~~ SSA (or more precisely, the optical radius) (Carmagnola et al., 2014) which is considered as the most important, morphological parameter of snow which can be measured ~~objectively in the field~~ by various techniques ~~in the field. Validations of the new model rely on experimental data for the density and the specific surface area, which can~~.

Besides SSA, there is certainly a demand for higher-level morphological metrics to characterize snow microstructure. Various physical properties have been shown to be influenced by morphological characteristics beyond the SSA, e.g. thermal conductivity (Löwe et al., 2013) by anisotropy, the

extinction of light (Libois et al., 2013) by grain shape, the scattering of microwaves by correlation lengths (Wiesmann et al., 1998) or confined compression of new snow by the Euler characteristic (Schleef et al., 2014b). The Euler characteristic is a topological metric for the connectivity of the structure (Michelsen et al., 2003). One one hand it might be regarded as a generalization of the grain-based concept of a coordination number (Lehning et al., 2002) to arbitrary 3D microstructures. On the other hand, the Euler characteristic is also exactly related to the average Gaussian curvature. The Euler characteristic thus constitutes a link to structure characterization in terms of full distributions of interfacial curvatures as a high-level morphological metric. This has e.g. been recently used to reveal details of temperature gradient metamorphism (Calonne et al., 2014). These recent advances in microstructural insight are indeed necessary and important, but none of these higher-level morphological metrics have been implemented in snow models yet, not to mention the difficulties to measure them by methods other than micro-computed tomography (μ CT). In the absence of advances to include or alternatively measure higher-level metrics, the density and the SSA must still be considered as the most important microstructural parameters for ~~the aforementioned models current~~ snowpack models. A good representation of the time evolution these parameters is a minimum requirement for these models. To reveal shortcomings of present models there is a need to bridge from laboratory-based techniques (e.g. μ CT) to field techniques to facilitate the validation of basic processes like metamorphism and densification under a wide range of environmental conditions.

~~Previously~~ From the perspective of laboratory experiments, some progress has been recently made to understand the physical mechanisms underlying new snow densification and metamorphism within creep experiments (Schleef and Löwe, 2013). The results indicate that the evolution of the SSA occurs ~~rather~~ autonomously without being affected by the concurrent densification. The experiments were carried out for a single type of ~~nature identical snowmaker~~ new snow at a single temperature.

~~This~~ However, this small range of experimental conditions is ~~however~~ of only limited ~~, direct~~ use for the aforementioned applications ~~and the validation of models~~. To cover a wide range of ~~natural environmental~~ conditions for snow types and temperatures, applications are ~~naturally~~ interested in best fit behavior of large data sets which are essential benchmarks to validate and drive snow evolution models. ~~Data~~ From the perspective of field experiments, some data sets are available for well-aged seasonal snow (Dominé et al., 2007) and data of experiments which includes new snow at the beginning (Cabanes et al., 2002, 2003; Legagneux et al., 2003; Taillandier et al., 2007). But comparable data from in-situ experiments which monitor the evolution of the *same* sample of new snow at high temporal resolution is almost non-existent.

To fill this gap we present a comprehensive data set of ~~tomography~~ μ CT experiments for new snow densification and metamorphism covering various examples of natural and laboratory-grown new snow with a wide range of ~~crystal habits~~. ~~By carrying out~~ initial crystal morphologies. The primary goal of the present work is to provide laboratory-based experimental data for validation purposes. Our aim is to bridge from high-level laboratory experiments to the capabilities of field measurements

95 by assessing, if densification and metamorphism under isothermal conditions can be described by
the most important, yet available, parameters for snow models, namely the density, temperature,
overburden stress and the SSA. We focus on the SSA as the most important morphological metric
for snow microstructure. To make contact to the original idea of crystal classification we include a
qualitative characterization of our experiments in terms of crystal habit classes. To make contact to
recent high-level morphological metrics, we also analyze the Euler characteristic.

100 The outline of the paper is as follows. In section 2 we briefly summarize the methods for
the experiments and the analysis which have been previously published elsewhere (Schleef and
Löwe, 2013; Schleef et al., 2014a,b). We present in-situ creep experiments at different tempera-
tures and overburden stresses, and monitor the evolution of the main microstructural parameters,
the namely ice volume fraction ϕ_{ice} and the SSA, is monitored typically ϕ_i and SSA over one to
105 two days at a temporal resolution of 3 hours. A reference experiment over an entire week indi-
cates that this is sufficient to capture the main aspects of microstructural changes. As a generic
result for all parameters The results of the experiments are given in section 3. As an interesting
generic result, we consistently find an almost linear relation between the density and the specific
surface area, with different slopes, though, which depend on the specific conditions (section 3.2).

110 In the following we separately discuss the influence of temperature (section 3.3) and morphological
characteristics (section 3.4) on densification rate and SSA decrease rate. The different stress levels
give rise to particularities which are pointed out. In section 3.5 we address the combined effects
of all parameters on densification rate and SSA decrease rate. Based on this observation and our
generic relation between SSA and density and based on previous modeling ideas for the SSA and
115 densification rate we present we derive simple parametrizations for the microstructural evolution of
rate equation of SSA and density for new snow in terms of the most important parameters for snow
models namely ϕ_{ice} , yet available, parameters namely ϕ_i , SSA, temperature T and stress σ . The
influence of these parameters are discussed separately. To understand particularities of the results
we also analyzed the Euler characteristic as an additional parameter, which was recently employed
120 to interpret compression experiments of new snow. Our parametrization for the SSA is compared to
an existing parametrization (Taillandier et al., 2007) in section 3.5. Finally, we discuss our results in
section 4.

2 Methods

For the following isothermal tomography measurements and their analysis we refer to for an elaborate
125 description of the experimental details. For a self-contained presentation we summarize the main
steps of the method and outline differences or extensions to (Schleef and Löwe, 2013; Schleef et al.,
2014a,b).

All snow samples were prepared from fresh snow, which was either collected outside or pro-

duced with a machine in the cold laboratory (Schleef et al., 2014a), referred to as natural snow and snowmaker snow, respectively. An overview of all sets of experiments with their main characteristics is given in Table 1. The natural snow was collected just outside the cold laboratory in Davos, Switzerland, during the winters 2011/2012 and 2012/2013. ~~Only To minimize previous metamorphism, only~~ intense snowfalls at air temperatures below -2°C with a deposition time less than an hour were chosen ~~to minimize previous metamorphism~~. Immediately afterwards the snow was sieved (mesh size 1 mm) into sample holders of 18 mm diameter with 15 mm filling height. In between, photographs of sieved snow crystals were taken to capture the crystal habit. Each set of snow samples comprised several identically prepared samples which were stored in a freezer at ~~-60~~ -60°C to nearly ~~suppresses~~suppress metamorphism until the experiments (Kaempfer and Schneebeli, 2007). In total, 8 sets of snow samples from different natural snow falls and 6 sets from different snowmaker runs were prepared ~~which are listed in~~ (Table 1-

~~The-). In~~ Schleef and Löwe (2013) we have addressed the potential bias caused by different storage times. We found that no systematic change of the SSA and density during storage times of three weeks at -60°C in the SSA range of around 70 mm^{-1} could be measured by μCT . The storage influence observed for some samples (SSA: $\sim 2\%$, density: $\sim 5\%$) is generally small compared to the observed evolution during the experiments.

All experiments were conducted within at most 3 weeks after sample preparation. The respective sample was placed in the cold laboratory one hour before the first measurement for thermal equilibration. For some experiments (Table 1) a cylindrical weight, corresponding to a stress of 133, 215 or 318 Pa, respectively, was carefully put on the sample half an hour before starting the first measurement to analyze the influence of external stress. Stress values were chosen to mimic different potential bury depths of new snow inside the snowpack, the stress values correspond to bury depths of about 0-30 cm, given an average new snow density of 100 kg m^{-3} .

The measurements were conducted with a desktop computer tomograph (μCT 80, SCANCO medical) operated in a cold laboratory at isothermal temperatures of about -13 or -18°C . For a single set (no. 14, cf. Table 1) the temperature was varied systematically to higher values of about -3 and -8°C to investigate the influence of temperature. For these samples, the temperature was recorded during the whole experiment with a sensor (iButton device) in the sealing cap of the sample holder. All samples were kept undisturbed in the μCT during the whole experiment which took one or two days. In one case, the measurement was extended to an entire week. μCT scans of a fixed ~~volume~~ of 6.3 mm height (cylindrical) sub-volume in the middle of the ~~samples~~ sample with total height of 6.3 mm were conducted automatically with a time-interval of 3 hours. The nominal resolution was $10\text{ }\mu\text{m}$ voxel size and the energy 45 kV. One scan took about two hours. In total, 45 time series were measured leading to more than 600 μCT scans.

For the analysis, a cubic volume of 6.3 mm edge length was extracted for each measurement and segmented into a binary file of ice and air. From the resulting 3D images the ice fraction and the spe-

cific surface area was calculated (details in (Schleef and Löwe, 2013)). In the following the results are exclusively presented in terms of the the ice volume fraction ϕ_{ice} ϕ_i which is directly obtained from the μ CT. The volume fraction can be related to the snow density via $\rho = \phi_{ice} \rho_{ice} + \rho = \phi_i \rho_i$ with the temperature dependent density of ice $\rho_{ice} = 917 - 920 \text{ kg m}^{-3}$ $\rho_i = 917 - 920 \text{ kg m}^{-3}$ (0 to 170 -20°C) (Petrenko and Whitworth, 1999). For the SSA we use the definition as surface area per ice volume, which is related to the surface area per ice mass (SSA_m) by $SSA = \rho_{ice} \rho_i SSA_m$.

Though we mainly focus on the ice volume fraction and the SSA for the analysis we have additionally evaluated the Euler characteristic χ of the samples. The Euler characteristic provides information about the topology ~~of the samples~~ which has been proven useful to understand the evolution 175 of the snow microstructure under forced compression in a ~~microcompression~~ micro-compression device (Schleef et al., 2014b). The Euler characteristic $\chi = 2 - 2g$ is related to the interface genus g which is an indicator for the connectivity of a structure (Michelsen et al., 2003). The Euler characteristic ~~typical~~ typically assumes negative values, corresponding to high positive values of the interface genus. The higher the genus, the lower χ and the higher the number of ~~interparticle~~ inter-particle 180 contacts. We calculated the Euler characteristic from the integral geometric approach of Minkowski functionals outlined by Michelsen et al. (2003). In accordance to the calculation of the SSA as a surface area per *ice volume* we normalized the Euler characteristic χ by the ice volume.

For the isothermal tomography measurements and their analysis we refer to Schleef and Löwe (2013) for an elaborate description of the experimental details.

185 3 Results

3.1 Overview

The natural new snow samples ~~showed a high variability of their initial characteristics. The nature identical~~ show large variations in the initial values of SSA and density. The snowmaker samples also varied in their initial characteristics and parameters due to different temperature settings of the ~~snowmaker~~ 190 machine (Schleef et al., 2014a). Overall, the initial ice volume fractions ranged from about 0.05 to 0.12, the initial SSA values were in the range $62\text{-}105 \text{ mm}^{-1}$, and the initial χ values were between $-2 \cdot 10^5 \text{ mm}^{-3}$ and $-12 \cdot 10^5 \text{ mm}^{-3}$. The averaged initial values of ϕ_{ice} ϕ_i and SSA of each new snow type are listed in Table 1. The initial values had an influence on the settling, yielding a faster densification for a lower initial ϕ_{ice} ϕ_i and a faster SSA decay for a higher initial SSA, but also 195 variations of other parameters like temperature and stress led to a high variability.

As a starting point for our subsequent analysis we ~~demonstrate the variability in the bare~~ show the entire data for the temporal evolution of the ice volume fraction and the SSA for all samples in Figure 1 and Figure 2, respectively. Despite the variability, some trends are immediately visible, e.g. an influence of the initial SSA on the subsequent decay. However, other trends which may be 200 expected (e.g. a clear ordering of the densification rates according to the applied stress) are clearly

absent. A more detailed analysis of the individual influences is necessary.

For one randomly selected sample of natural snow at -13°C we extended the observation to a whole week. From the analysis we obtained the evolution of $\phi_{\text{ice}}-\phi_i$ and SSA at high temporal resolution, as shown in Figure 3. For the given example, no external stress was applied, but the
205 volume fraction $\phi_{\text{ice}}-\phi_i$ increased by more than 40% from an initial value of about 0.11. At the same time the SSA decreased from 77 mm^{-1} to 45 mm^{-1} . A widely confirmed decay law for the SSA (Legagneux, 2004; Flanner and Zender, 2006; Kaempfer and Schneebeli, 2007; Schlee and Löwe, 2013) is given by

$$\text{SSA}(t) = \text{SSA}(0) \left(\frac{\tau}{t + \tau} \right)^{1/n} \quad (1)$$

210 with the parameters τ and n . A fit to the SSA data is shown in Figure 3 with the parameters $\tau = 27\text{ h}$ and $n = 3.8$ ($R^2 > 0.99$).

For a visual demonstration of the microstructural evolution we combined sections of the 3D images (snow 5) to a time-lapse movie which is provided as supplementary material. The densification and coarsening is clearly visible in the movie and occurs in the absence of recognizable particle
215 rearrangements and the creation of new ~~interparticle contacts~~. ~~This is confirmed by the evolution of the Euler characteristic χ which increases monotonically with a decreasing rate. This behavior of the Euler characteristic is common for most experiments and expected for isothermal coarsening. This topological signature of coarsening is not even influenced in the presence of applied stresses. Some examples for the evolution of χ in one day are shown in Figure 7. For later reference we note~~
220 ~~that a few samples show a non-monotonic behavior of the Euler characteristic at the beginning of the experiment.~~ inter-particle contacts.

3.2 General relation between density and SSA

Despite the common trends in the evolution of the SSA and the density, there is an apparent variability of individual curves ~~of density and SSA~~ shown in the previous section, ~~the evolution~~. However,
225 the coupled evolution of both turns out to be governed by a generic feature. As suggested by Figure 3 the increase of the volume fraction $\phi_{\text{ice}}-\phi_i$ seems to “mirror” the SSA decay. If the ice volume fraction $\phi_{\text{ice}}-\phi_i$ is plotted versus the SSA for all series (Fig. 4) an almost linear relation between both is consistently revealed irrespective of the experimental conditions. Except for one sample, which showed no densification at all, all other series of measurements can be fitted to ~~an~~ the empirical linear
230 relation ~~$\phi_{\text{ice}} = a \cdot \text{SSA} + b$~~ $\phi_i = a \cdot \text{SSA} + b$ with coefficient of variation $R^2 > 0.94$. The fit parameters vary in the range $a = [-2 \cdot 10^{-3}, -0.2 \cdot 10^{-3}]$ and $b = [0.08, 0.26]$ depending on applied stresses, temperatures or crystal habits, however, not in an apparent ~~systematic way~~, systematic way, as shown in Figure 4. We note that likewise a logarithmic law ~~$\ln(\phi_{\text{ice}}) = a' \cdot \text{SSA} + b'$~~ $\ln(\phi_i) = a' \cdot \text{SSA} + b'$
235 $R^2 > 0.93$. This logarithmic dependence was suggested by Legagneux et al. (2002); Dominé et al. (2007). The difficulty of discerning a logarithmic from a linear relation is not surprising since

$\ln(x) \approx -1 + x$ for values x close to one where both models seem to be equally valid. A detailed analysis of the experimental parameters on the SSA evolution and the densification will be carried out below.

240 3.3 Influence of temperature

To investigate the influence of different (isothermal) temperatures we measured the settling for one set of samples (snow 9-14 in Table 1) at ~~3~~ three different laboratory temperatures. The temperature of the samples was recorded continuously during the experiments resulting in mean values of -3.1°C , -8.3°C and -13.4°C . Even though additional fans ~~are~~ were mounted inside the μCT to minimize
 245 temperature fluctuations, the temperature changed during each scan by up to $\pm 0.5^\circ\text{C}$ due to the heating of the X-ray tube. In addition, the defrosting cycles of the cold laboratory heat exchanger caused small changes of the temperature twice a day. In total, the temperature fluctuations were at maximum $\pm 0.6^\circ\text{C}$ during one day, with the ~~highest~~ largest changes for the mean temperature of -3.1°C . For each temperature, we conducted one series without a weight on the sample and another
 250 one with a weight corresponding to a stress of 133 Pa and analyzed the density and the SSA.

3.3.1 Densification rate

The initial ice fractions of the samples were about 0.06-0.09. For the samples without applied stress almost no densification was observed within one day. Therefore a clear dependency on the temperature could not be obtained from the data of these samples. In contrast, the series with an
 255 applied stress of 133 Pa showed a significant, steady densification of 27%-48% per day which is clearly influenced by the temperature. The temperature influence of the densification of snow is often described by an Arrhenius law (Bader, 1960; Arnaud et al., 2000; Kirchner et al., 2001; Delmas, 2013)

$$\frac{\dot{\phi}_{\text{ice}}/\phi_{\text{ice}}}{\dot{\phi}_{\text{i}}/\phi_{\text{i}}} = \nu \exp\left(-\frac{E}{k_B T_K}\right) \quad (2)$$

260 with a rate constant ν , an activation energy E , the Boltzmann constant k_B and the temperature T_K in Kelvin. From the differences of the ice volume fraction between successive time steps we obtain the experimental densification rates. Following the Arrhenius law, the mean densification rates per hour for each series are plotted against the inverse temperature in Kelvin in Figure 5. The horizontal error bars result from the measured temperature fluctuations whereas the vertical errors bars indicate the
 265 maximum deviations from the mean values. By fitting the results to Eq. (2) we find the parameters $\nu = 4.8 \cdot 10^8 \text{h}^{-1}$ and $E = 0.56 \text{eV}$ ($R^2 = 0.49$) for the experiments with a stress of 133 Pa. The same fit for the experiments without stress yields $\nu = 2.8 \text{h}^{-1}$ and $E = 0.16 \text{eV}$ ($R^2 = 0.99$), however, there was only a marginal change of the density.

3.3.2 SSA decrease rate

270 The initial SSA of the samples ~~was ranged~~ between 70-78 mm⁻¹. For all samples a steady decay of 12-31% in one day could be measured. Figure 6 shows the mean SSA decay per hour with error bars calculated in the same way as described for the ice fraction evolution. The SSA decay increased significantly with higher temperatures. At a temperature of about -13°C the decay was almost independent of the applied stress. In contrast, for higher temperatures the experiments with a stress of
275 133 Pa showed an accelerated rate of SSA decay. The temperature influence can be best described with an empirical linear relation $\dot{SSA} = \alpha T + \beta$ with the parameters $\alpha = -0.02$ and $\beta = -0.62$ ($R^2 > 0.99$) for the experiments with stress ~~$p=0\sigma=0$~~ , and $\alpha = -0.04$, $\beta = -0.99$ ($R^2 = 0.99$) for ~~$p=133\sigma=133$~~ Pa. This is valid if the temperature is given in °C and \dot{SSA} in units mm⁻¹h⁻¹. In Figure 6 the experiments at higher temperatures and ~~$p=133\sigma=133$~~ Pa have a disproportionate
280 error on the SSA rate, which is caused by a much higher SSA difference between the first two measurements of the time series. By neglecting the first measurement, the difference of the SSA rate at high temperatures between the experiments with and without applied stress would only be small.

The particularity of the first time step is ~~partly~~ revealed by the Euler characteristic, which is ~~shown for $T \approx -3^\circ\text{C}$ analyzed below.~~

285 3.4 Influence of other morphological properties

3.4.1 Euler characteristic

A few selected examples for the evolution of the Euler characteristic χ during one day are shown in Figure 7. For most experiments, the Euler characteristic χ increases monotonically with a decreasing rate. In these cases the rate increased slightly with increasing temperature, but an influence of
290 external stress was not observed. This is shown for one example (snow 9) in Figure 7. ~~The measurements~~. For some experiments, at higher temperatures, this monotonic behavior of the Euler characteristic disappears. The measurement without applied stress ~~show~~ (snow 14, -3°C, $\sigma = 0$ Pa) shows a monotonic increase, similar to the other experiments at lower temperatures, similar to the evolution of the ~~one-week measurement one-week measurement (snow 5)~~ and similar to the
295 results for the other experiments, including those described by experiments from Schleef and Löwe (2013). ~~For the samples analyzed here, the rate increased slightly with increasing temperature. The measurement with a stress of (snow 9). However, if the stress is changed to 133 Pa however showed a different behavior. Within the first 3 hours between the first and the second measurement, (snow~~ 14 at -3°C, $\sigma = 133$ Pa) a different non-monotonic evolution of the Euler characteristic decreases
300 significantly, corresponding to an increase of the number of interparticle contacts. After that at the beginning of the experiment is observed. After this initial phase, the connectivity decreased again monotonically (i.e. increase of χ) similar to the evolution of the corresponding experiment without applied stress. The rate was however slightly lower. Such a significant decrease of the

305 Euler characteristic within the first 3 hours between the first and the second measurement has been observed only for a few measurements, predominantly at higher temperature. This decrease of the Euler characteristic corresponds to an increase of the number of inter-particle contacts, which contributes to the decrease of the SSA (Schleef et al. (2014b)). These cases gave rise to the larger error in the SSA rate for higher temperatures in Figure 6.

3.5 ~~Influence of crystal habit~~

310 3.4.1 Crystal habit

Finally we turn to apparent visual differences in the ~~crystal habit, and their possible influence on the settling morphology of the crystals~~. From the photographs we ~~could compare~~ compared the crystal habits of our samples to the classification of natural snow crystals (Kikuchi et al., 2013), as listed in Table 1. In most cases we observed broken parts of the respective crystal types, which ~~are likely~~ caused by the ~~might be caused by~~ sieving. But also wind can lead to broken crystals in nature, and we could still identify the original crystal for the classification. An unambiguous classification for each snow sample was however not possible, because each sample contained a mixture of different ~~crystals~~ habits. This was particularly the case for natural snow. For some samples, however, specific crystal habits dominated ~~the shape~~.

320 Figure 8 shows two examples of natural snow samples with a photo of the prominent crystal habit and the corresponding μ CT image of the initial structure. The sample ~~at bottom~~ (Figure 8, bottom) is the one with the evolution shown in Figure 3 (snow 5 in Table 1), with dominant crystal habit of skeletal columns with scrolls (C3c) and combinations of columns and bullets (A1a). For comparison we picked ~~a sample (top in another sample~~ (Figure 8, top) which had almost the same initial ice fraction (snow 2 in Table 1) but a different dominating crystal habit (broad branches, P2b). This sample was unique since no densification at all could be measured within two days at -18°C, in contrast to the previous sample (snow 5) which showed a densification of about 18% ~~in the same time within the same span~~ at -13°C. However, the ~~high-large~~ difference cannot be explained by the temperature, because for all other samples there is no trend for the densification between 325 the measurements at -13 or -18°C. There are also other samples with smaller differences in the densification rates for the same volume fraction and the same temperature and stress. In contrast, for the SSA decay rate no clear influence of the crystal habit has been found. In most cases the SSA evolution at the same temperature is identical for the same SSA values.

3.5 Combined influence of stress, temperature and morphology: Parametrizations for rate equations

335

3.5.1 SSA decrease rate

To provide an overall quantitative description of the SSA decrease rate with time and the densification rate which accounts for all measured quantities, we set up a simple parametrization based on previous our observations and existing models in concepts from literature.

340 ~~To this end we note that~~

3.5.1 SSA decrease rate

For the SSA decrease we start from the widely used power law from Eq. given in Eq. (1). This is motivated by the very good agreement of Eq. (1) for the one-week measurement (Figure 3) even though also other functional forms are discussed in literature (Taillandier et al., 2007). To proceed, we note that Eq. (1) is the solution of the differential rate equation

345

$$\dot{SSA} = A \cdot SSA^m \quad (3)$$

if the parameters from Eq. (1) are chosen according to $n = m - 1$ and $\tau = -\frac{1}{A^n} SSA(0)^{-n}$. The proportionality of τ to $SSA(0)^{-n}$ is in accordance with the derivation from Legagneux (2004). On the other hand our observations from Section section 3.3 indicate a linear influence of the temperature on the SSA decrease rate on the temperature, while. But no influence on the applied stress has been observed during coarsening, except one case discussed in section 3.3.2. In addition, we have observed that for some cases the initial SSA rates ~~for some cases~~ are influenced by topological changes during densification (Fig. 7), as described by the Euler characteristic χ (section 3.4.1). In summary we chose the following form for the statistical model

350

$$\dot{SSA} = (a + bT) SSA^m + c\dot{\chi} \quad (4)$$

355

with the parameters a , b , c and m . Incorporating the topological influence $\dot{\chi}$ in an additive way in Eq. (4) is thereby in accordance to the relation found by compression experiments (Schleef et al., 2014b). ~~With that~~ Thereby, we consider that the SSA is not only affected by metamorphism but also by the number of contacts during settling between the ice grains. Crucial topological changes, i.e. the creation of new contacts within the structure, occurred only for a few samples at the beginning of the series of measurements.

360

A fit of Eq. (4) to the SSA rates obtained from the difference $\Delta SSA / \Delta t$ of successive measurement within typically three hours for our complete data set yield $a = 2.9 \cdot 10^{-7}$, $b = 9.5 \cdot 10^{-9}$, $c = -3.5 \cdot 10^{-3}$ and $m = 3.5$ with ~~$(R^2 = 0.83)$~~ . ~~This is valid for temperature given (T in °C, the SSA in units of SSA in mm^{-1} and $\dot{\chi}$ in units mm^{-3}).~~ The scatter plot between modeled and measured SSA rates is shown in Figure 9.

365

If we neglect the measurements where noticeable topological changes ($\dot{\chi} < 0$) occurred, which was only the case for ~~10~~ten samples for the first measurements, we could ~~even~~ simplify the model to

$$370 \quad \dot{SSA} = (a' + b'T)SSA^{m'}, \quad (5)$$

leading to fit parameters $a' = 1.1 \cdot 10^{-6}$, $b' = 3.1 \cdot 10^{-8}$ and $m' = 3.1$. In this case we obtain an even improved performance ($R^2=0.87$). This is particularly interesting, given the practical ~~difficulty~~ impossibility to measure the Euler characteristic without tomography.

3.5.2 Densification rate

375 A parametrization for the densification rate ~~$\dot{\phi}_{ice} \phi_i$~~ for all measurements turns out to be more complicated than for \dot{SSA} , since ~~$\dot{\phi}_{ice} \phi_i$~~ is not only influenced by temperature and the initial value ~~$\phi_{ice,0}$~~ $\phi_{i,0}$ but also by the stress and the crystal habit, as described before.

To motivate a model which aims to fit the entire data we start from the common stress dependence of the strain rate for visco-plastic flow of polycrystalline ice which is commonly described by Glen's
380 law for secondary creep, $\dot{\epsilon} = A\sigma^k$ (Petrenko and Whitworth, 1999). A similar form is believed to be valid for snow (Kirchner et al., 2001). In a one-dimensional system, the strain rate $\dot{\epsilon}$ can be taken as the relative densification rate ~~$\dot{\epsilon} = \dot{\phi}/\phi$~~ $\dot{\epsilon} = \dot{\phi}_i/\phi_i$ (cf. also Schlee and Löwe (2013)) leading to

$$\dot{\phi}_{ice} \phi_i / \phi_{icei} = A\sigma^k \quad (6)$$

with a constant A containing the rate of the process.

385 On the other hand we have empirically observed that the volume fraction is almost linearly related to the ~~specific surface area~~ SSA (section 3.2). Hence we chose the rate in Eq. (6) to be determined mainly by the SSA rate ~~$A = B\dot{SSA}$~~ , $A = B\dot{SSA}$, and end up with

$$\dot{\phi}_{ice} \phi_i / \phi_{icei} = B\dot{SSA}\sigma^k \quad (7)$$

for our parametrization model, which includes two parameters, B and k . We note that integrating
390 Eq. (7) in fact implies ~~$\ln(\phi_{ice}) \sim SSA$~~ $\ln(\phi_i) \sim SSA$ and not a linear dependence. This is however in accordance with the result from ~~Section 3.2~~ section 3.2, where the logarithmic or the linear relation are indistinguishable. Thus Eq. (7) constitutes a reasonable trade off and naturally includes a dependence of the densification rate on the density itself.

A fit of Eq. (7) to the densification rates ~~obtained from the difference of $\Delta\phi_i/\Delta t$ obtained from~~
395 successive measurements within typically three hours for our complete data set yields $B = -6.6 \cdot 10^{-3}$ and $k = 0.18$. This is valid for stresses given in units of Pa and \dot{SSA} in units $\text{mm}^{-1}\text{h}^{-1}$. We note that samples without a weight are assigned a remaining, non-zero stress of 5 Pa caused by the small but non-negligible overburden of the overlying snow inside the μCT sample holder on top of the evaluation cube. The same value was chosen by Schlee and Löwe (2013). The scatter plot
400 between modeled and measured densification rates is shown in Figure 10, yielding $R^2 = 0.82$.

~~We note that~~ As suggested by the results from (Schleef et al., 2014b), the Euler characteristic has an influence on the densification by discerning different connectivities. Accordingly, a slight improvement of the parametrization (7) ~~might be slightly improved~~ is obtained by including the Euler characteristic via

$$405 \quad \dot{\phi}_{\text{icei}} / \phi_{\text{icei}} = (B' \sigma^k + C' \chi) \text{SSA} \quad (8)$$

which yields $R^2 = 0.85$. In contrast to Eq. (4), where the additive dependence of the SSA decrease on the Euler characteristic was motivated by process insight (Schleef et al., 2014b), the inclusion of χ in (8) is purely empirical.

3.6 Comparison to an existing parametrization

410 Finally we compare our parametrization (5) for the SSA evolution to an existing parametrization from Taillandier et al. (2007), who derived a parametrization $\text{SSA}_{\text{T2007}}(t, T, \text{SSA}(0))$ (Eq. 13) in their paper) for the isothermal and quasi-isothermal evolution of the SSA with time t for given temperature T and initial value $\text{SSA}(0)$. The parametrization was derived from SSA measurements which were conducted by the Brunauer–Emmett–Teller (BET) method of gas adsorption, with new
 415 snow samples collected after snowfall. With respect to the involved parameters, this is exactly equivalent to our parametrization $\text{SSA}_{\text{S2014}}(t, T, \text{SSA}(0))$ which is obtained from integrating Eq. (5). To compare the overall trends of both parametrizations, we have computed the SSA difference after 48h, $\Delta \text{SSA}_X(48h) = \text{SSA}_X(48h, T, \text{SSA}(0)) - \text{SSA}_X(0h, T, \text{SSA}(0))$ for both formulations $X = \text{T2007}, \text{S2014}$ to provide a measure of the averaged SSA decay rate on the first day after snowfall.
 420 To use realistic values for $(T, \text{SSA}(0))$ from real data-sets, we have evaluated the difference $\Delta \text{SSA}_X(48h)$ for the present data set (45 tuples of $(T, \text{SSA}(0))$), the isothermal experiments 1-9 from (Taillandier et al., 2007) (9 tuples), and the experiments 1-5 from (Legagneux et al., 2003) (5 tuples). The results are shown in Figure 11. A clear deviation from the 1:1 line is observed. In general our parametrization of the SSA decay rate is biased low compared to (Taillandier et al., 2007). This
 425 bias remains, also if $\Delta \text{SSA}_X(t)$ is evaluated for other times t . However, the parametrization T2007 based BET measurements and the parametrization S2014 based on μCT measurements are clearly correlated. In both cases the major difference of the SSA decrease rate is caused by the initial value $\text{SSA}(0)$.

4 Discussion

4.1 Main result

We start the discussion ~~from with~~ the parametrization of the SSA and the densification for new snow under isothermal conditions (Section section 3.5). ~~We note that our experiments focused only on new snow with low density and high SSA and most of our results are probably not valid for denser snow.~~

The parametrizations are motivated by available models for the SSA (Legagneux, 2004) and Glen's
435 law for creep of polycrystalline ice (Petrenko and Whitworth, 1999). ~~Most Conceptually,~~ current
snowpack models (Vionnet et al., 2012; Jordan, 1991; Bartelt and Lehning, 2002) use a similar
approach for the densification, but ~~are still~~ based on traditional grain size ~~concerning to characterize~~
the microstructure. ~~Recently~~ Only recently, the model Crocus was ~~modified to use directly SSA to~~
~~express the microstructural properties re-formulated~~ (Carmagnola et al., 2014) to use SSA as the
440 simplest, objective, morphological metric directly.

Our experiments focused only on new snow with low density and high SSA and most of our results
are probably not valid for denser snow. In contrast to denser snow under isothermal metamorphism,
we found that the densification rate is directly related to metamorphism via the SSA decrease
rate. This is reflected by the consistent linear variation of the ice volume fraction with the SSA (Fig. 4).
445 This observation was implemented in the parametrization by a prefactor in the densification rate
which is proportional to the SSA rate. We have set up the parametrization for the densification in
a way to guarantee that both evolution laws are only dependent on the quantities ~~ϕ_{ice}~~ ~~ϕ_i~~ (or the
density), the stress σ , the specific surface area SSA and the temperature T to best fit the entire,
available data of new snow. ~~Thereby~~ These quantities are directly available in snowpack models
450 and Eqs. (5, 7) provide a closed set of empirical, microstructural evolution equations for the density
and the SSA under isothermal conditions. Both microstructural parameters, SSA and density can be
obtained in the field ~~, also~~ without the use of tomography (Matzl and Schneebeli, 2006; Gallet et al.,
2009; Arnaud and Picard, 2011).

~~The data set provides a comprehensive benchmark to validate new parametrization of snowpack~~
455 ~~models in terms of SSA and density. Our new parametrization will also be useful to predict the~~
~~evolution of the albedo, as information about the evolution of SSA in new snow is scarce~~

4.2 Comparison to other parametrizations

Our comparison with the parametrization from (Taillandier et al., 2007) (section 3.6) has revealed
that our parametrization (4) always underestimates the average SSA decay in 48h for given temperature
460 and initial SSA when compared to their result (Figure 11). Different explanations for these differences
are possible. First, both parametrizations are based on different time scales. Our measurements
comprise only the evolution within typically 2 days with high temporal resolution of 3h. In contrast
(Taillandier et al., 2007) focuses on the evolution up to 100 days, where the first measurement
was only conducted after 24 hours, and the parametrization naturally includes higher statistical
465 weight for longer times. Second, differences in the magnitude of temperature fluctuations might
have an influence. If the isothermal experiments from (Taillandier et al., 2007) were subject to
temperature fluctuations larger than our accuracy of $\pm 0.6^\circ\text{C}$, these fluctuations might cause an
increase of the SSA decay rate according to mechanisms mentioned in (Pinzer and Schneebeli,
2009). A quantitative estimate of this effect is however not yet possible. Third, a systematic error

470 of the μ CT measurements compared to BET measurements used in (Taillandier et al., 2007) at these
very high SSA values could not be ruled out. The comparison of BET and μ CT from (Kerbrat et al.,
2008) has not revealed a systematic bias, though, but the uncertainty between both methods clearly
increases at high SSA values. For very high SSA values, our μ CT measurements with voxel size
of $10\mu\text{m}$ are at the limit of the resolution. Ideally, remaining uncertainties about absolute values of
475 very high SSA should be further investigated within dedicated inter-comparison experiments.

The origin of the remaining differences could not be convincingly explained. However, the trends
from Figure 11 obtained from the two parametrizations, which were based on different experimental
techniques (μ CT vs BET), are highly consistent. This motivates to measure the SSA of new snow
also by other, less demanding techniques in the field. This will help to explore the influence of the
480 initial SSA on new snow densification and improve the performance of snowpack models. Below
we discuss the particularities of the SSA decrease rate and densification rate in view of the involved
parameters.

4.3 SSA decrease rate

Our simple parametrization for the SSA change (4) ~~yields~~ yielded good agreement for almost all
485 of our measurement data. The exponent m obtained from the fit must be compared to n from the
widely used Eq. (1) via $n = m - 1$, yielding $n = 2.5$. As already outlined by (Schleef and Löwe,
2013), the precise value of n is difficult to estimate, if the duration of the experiment is similar
to τ , which is typically in the order of one day. This is confirmed by the ~~one-week measurement~~
~~which allows one-week measurement which allowed~~ a better estimate of the fit parameters in Eq. (1).
490 The obtained exponent $n = 3.8$ ~~agrees~~ agreed well with the results of Legagneux (2004) who found
 $n = 3.4 - 5.0$ at a temperature of -15°C . In contrast, the results of the short time measurements did
not lead to a conclusive estimate for n . Also the fits to the 2 day time series by Schleef and Löwe
(2013) gave higher values of n and only an adapted combination of all series resulted ~~to in~~ in a similar n
of about 3.9. However the value $n = 2.5$ indicates that, even for short times, the SSA decrease rate is
495 dominantly influenced by the present value of the SSA in a non-linear way. It is generally believed
that the value of n is also influenced by temperature, potentially caused by different underlying
mechanisms of mass transport (Vetter et al., 2010; Löwe et al., 2011). In view of the difficulties of
estimating n for the short time series, we have restricted ourselves to an inclusion of the temperature
dependence into the prefactor in Eq. (4) to account for the acceleration of metamorphism at higher
500 temperatures (Fig. 6).

We have previously observed that the SSA evolution ~~is was~~ is in fact independent of the densification
~~, or respectively or~~ or the applied stress, respectively (Schleef and Löwe, 2013). This ~~is was~~ is confirmed
here for all experiments conducted at ~~about lower temperatures of~~ about -13°C or -18°C (cf Table 1) ~~which~~
~~can thus be generalized to all examined new snow types. Furthermore, in general. This behavior~~
505 seems to be generally valid for all examined types of new snow. In addition, no difference could be

observed between the evolution of sieved, natural new snow ~~samples~~ and snowmaker snow, which is in agreement to the results presented by Schlee et al. (2014a). The reason for the negligible stress dependence at low temperatures is that coarsening is the only relevant process. In these cases the Euler characteristic is a monotonic function with time (this is further explained below). At higher
510 temperatures we have also observed cases where the Euler characteristic initially decreased. This is a clear indicator of structural re-arrangements and newly formed ice-ice contacts which contribute to the SSA decrease (Schlee et al., 2014b). This was however observed only for a few cases. If present, the structural re-arrangements and their impact on the SSA do depend on stress. This was revealed by the two (out of 584) Δ SSA outliers in Figure 9. These are the first values of the series of
515 measurements with an applied stress of 133 Pa at temperatures of -3°C and -8°C. Exactly for these measurement a significant direct influence of the applied stress on the SSA evolution was observed which is not captured by the model (4). The data is however too limited to investigate this effect in greater detail. Apart from that, the parametrization Eq. (4), which is solely based on common snowpack model parameters, is well suited for modeling the SSA decrease of new snow.

520 4.4 Densification rate

The analysis of ~~$\dot{\phi}_{ice}$~~ ~~ϕ_i~~ is based on the observation of the almost linear relation between the evolution of ~~$\dot{\phi}_{ice}$~~ ~~ϕ_i~~ and SSA for each series of measurement (Fig. 4). Measurements of Legagneux et al. (2002); Dominé et al. (2007) ~~showed~~ show a logarithmic relation between density and SSA, which ~~was~~ is however derived from independent measurements in a seasonal snowpack and ~~covered~~ covers
525 much wider SSA and density ranges. As outlined in ~~Section~~ section 3.2 a logarithmic relation for each of our series of measurement would also be possible here, and the linear relation might only be an approximation for short observation times. It is however not the functional form which is worth mentioning, it is rather the fact that the density evolution and the SSA evolution are intimately related.

530 In contrast to the SSA rate, a direct temperature dependence of the densification rate is less pronounced in the overall behavior ~~of the densification rate. This originates.~~ This stems from the fact that the main impact of densification comes from metamorphism itself via the SSA rate in Eq. (7), which implicitly contains a temperature dependence as discussed in the previous section. In general ~~we would also expect,~~ one may expect also an explicit temperature dependence for the creep
535 rate A in Eq. (7). The ~~dedicated~~ Arrhenius analysis of the temperature dependence for one of the sets for two stress values (Fig. 5) ~~reveals~~ revealed that the densification is almost negligible for the case without weight. For the experiments with applied stress a faster rate of ~~$\dot{\phi}/\phi$~~ ~~ϕ_i/ϕ_i~~ could only be observed at about -3°C. The Arrhenius fit (2) yields an activation energy in the same order of magnitude as known for different possible processes in ice (about 1 eV, Kirchner et al. (2001) and
540 references therein), but the limited amount of data with just one series of measurement at -3°C and 133 Pa did not allow for conclusive parameter estimates. Obtaining reliable data for higher tempera-

tures by desktop tomography is generally difficult, since the timescales of the fast structural changes of new snow are already in the order of the scanning ~~intervals~~times; ~~image artifacts arise~~. Due to this ~~technical limitation~~, most experiments were conducted at -13°C or -18°C where no general trend for
545 a faster densification at higher temperatures could be observed.

4.5 ~~Remaining uncertainties~~The influence of other morphological parameters

Besides the most important ~~parameters~~microstructural parameters, density and SSA, we have also ~~classified crystal habits to make contact to traditional characterization of crystal morphology and~~ calculated the Euler characteristic ~~to provide additional confidence for the interpretation of the results.~~
550 ~~We~~, to make contact to more advanced morphological metrics.

4.5.1 Crystal habit

~~For selected examples, the classification of crystal habits has helped to empirically interpret experimental scatter. The examples in Figure 8 have shown that densification can easily differ by about 18%, which can not be explained by the temperature difference alone. Differences in crystal habit and their influence on the densification rate are not captured by our parametrization, which contains the SSA as the only morphological parameter. It seems unlikely that SSA is a sufficient morphological description of new snow type in the densification rate, as suggested by Eq. (7). However, for most of our measurements, the parametrization Eq. (7) works reasonably well, even though only two fit parameters are involved. In contrast, for the SSA evolution the crystal habit does not have an evident influence. Similar decay rates were found for samples with similar initial SSA but different crystal habits. Overall, the classification in terms of crystal habits was not very helpful, some influence of the habit might be acknowledged, but future effort should rather aim at other quantitative, morphological parameters to explain the remaining scatter.~~
555
560

4.5.2 Euler characteristic

~~As suggested by recent compression experiments of new snow (Schleef et al., 2014b), the Euler characteristic might be a candidate morphological parameter to better interpret the evolution of SSA and density. Quantitatively, we have seen that the inclusion of the Euler characteristic in the parametrizations with Eqs. (4) and (8) only makes a slight difference for the very initial stage where some particle rearrangements re-arrangements are noticeable. In general we observed for~~ For the
565 majority of samples ~~that we observed a monotonic increase of~~ the Euler characteristic ~~showed a monotonous increase~~, or equivalently a ~~monotonous-monotonic~~ decrease of the number of contacts. This is expected ~~from coarsening as a consequence of coarsening of bicontinuous morphologies alone~~ (Kwon et al., 2007) ~~due to the reduction of finer parts of the structure, where contacts, made of fine filaments, disappear~~. For a highly porous material like new snow, the slow creep deformation
570 considered here does not cause significant structural re-arrangements and new contacts. This is

confirmed by the visual inspection of the deformation from the movie (cf. supplementary material).
~~The inclusion of the topology does not seem to be essential to describe isothermal densification and metamorphism of new snow. Solely for~~ For a few experiments ~~we observed~~, the Euler characteristic signaled an increase of the connectivity at the beginning. This was the case for samples with faster
580 creep rates due to higher temperature, higher ~~stress and~~ stresses or a very tenuous ~~structure~~. ~~In this case~~ structures. In these cases, an influence on the evolution of SSA and ϕ_{ice} can be observed. ~~But in general these~~, which is not captured by Eqs. (4) and (8). However, initial structural re-arrangements stabilize quickly. This is consistent with ~~the mechanism of~~ externally forced re-arrangements in deformation controlled compression experiments (Schleef et al., 2014b), in a less
585 pronounced way, though.

~~Another origin of scatter of the model is revealed by the two (out of 584) Δ SSA outliers in Figure 9. These are the first values of the series of measurements with an applied stress of 133 Pa at temperatures of -3°C and -8°C . Exactly for these measurement a significant direct influence of the applied stress on the SSA evolution was observed which is not captured by the model. The data is~~
590 ~~however too limited to investigate this effect in greater detail. Apart from that, Eq. seems to be well suited for modeling the SSA change of new snow.~~

~~For most of our measurements, Eq. seems to describe the densification reasonably well, even though only two fit parameters are involved. A remaining uncertainty comes from differences in crystal habit. The examples in Figure 8 have shown that densification can easily differ by about~~
595 ~~18, which can not be explained by the temperature difference alone. These differences in crystal habit and their influence on the densification rate are not captured by our analysis. It seems unlikely that SSA is a sufficient geometrical description. Overall, the inclusion of the Euler characteristic as additional morphological parameter does not seem to be crucial for isothermal densification and metamorphism of new snow~~ type in the densification rate, as suggested by Eq. (7). We note however,
600 ~~that the crystal habit does not show an evident influence on the SSA evolution for samples with similar SSA values and different habits.~~

, at least for lower temperatures. However, the Euler characteristic has clearly helped to identify situations where the evolution was not only governed by coarsening alone. In common snowpack models ~~the shape~~, additional morphological information beyond SSA is empirically included in the
605 dendricity parameter (Vionnet et al., 2012; Lehning et al., 2002). ~~The inclusion of such a parameter seems to be crucial, even though it is~~ This parameter is actually not sufficiently exploited yet since new snow is commonly always assigned the same dendricity, irrespective of the ~~new snow type~~ actual morphology of the crystals. The inclusion of an additional, objective parameter seems crucial, if the remaining scatter in SSA decrease rate and densification rate is an issue. To improve the under-
610 standing of new snow densification beyond Eq. (7) it seems important to replace also the dendricity by an objective microstructural parameter which captures relevant differences in crystal ~~habit or shape~~ morphology. A candidate might be the anisotropy parameter Θ as pursued by Löwe et al.

(2013); Calonne et al. (2014) to reduce the scatter in the data for the thermal conductivity. A direct application of the methods from Löwe et al. (2013) is however not possible, since the correlation
615 function for new snow can certainly not be approximated by a simple exponential form. A potential generalization of the methods from Löwe et al. (2013), tailored to the evolution of new snow, ~~is left for~~ will be addressed in future work.

5 Conclusions

We have ~~shown that the rate of SSA decrease and thereby the SSA itself has probably the most~~
620 ~~dominant influence on isothermal new snow densification. It is inevitable that the assumption of isothermal conditions for the new snow deposit is only occasionally and approximately valid in nature. But given the experimental difficulties of both, characterizing the true thermal driving of the near surface snow in the field and reproducing these conditions within tomography experiments, we believe that our isothermal experiments provide a valuable reference data set~~ compiled a large data
625 set of 45 time series (and a total of 600 μ CT measurements) of in-situ experiments of new snow densification and metamorphism by μ CT. For a quantitative characterization of all experiments, we have derived a parametrization for the SSA decrease and densification rate which performs reasonably well ($R^2 = 0.87, 0.82$, respectively) for the entire data set of ~~45 time series (and a total of 600 μ CT measurements)~~ of new snow experiments which were evaluated for the present anal-
630 ysis. ~~Though advanced microstructural characteristics~~ The parametrization is only based on the parameters SSA, density, temperature, and stress, which are already available in current snowpack models, and which can be easily measured in the field. With these parameters, the main influences of metamorphism and densification of new snow can be quantitatively described. Advanced morphological metrics like the Euler number characteristic give additional insight in the interpretation of the densification
635 ~~experiments, it is~~ SSA and density evolution, the parametrizations have however not improved significantly upon inclusion of this parameter. This might be different for high temperatures, close to 0°C, where only few data is available due to the experimental limitations of μ CT imaging for fast microstructural changes. It is however likely that an additional shape parameter morphological parameter besides the SSA is required to reduce the remaining scatter in the description of new
640 snow densification. This will require additional, theoretical work to guide the choice of a relevant parameter and suggest functional forms for parametrizations which improve existing ones.

The comparison of our parametrization for the SSA (as a function of time, temperature and initial SSA) with a formally equivalent one from (Taillandier et al., 2007) has revealed a bias in the absolute values of SSA decrease, the trends of both formulations are however highly consistent.
645 These trends can be probably also reproduced by simpler SSA retrieval methods (other than μ CT or BET) which are more convenient to use in the field. This is important for further validation of snowpack models. We have shown that the rate of SSA decrease and thereby the SSA itself has

probably the most dominant influence on isothermal densification of new snow. Hence, monitoring
the SSA for operational purposes might greatly help to constrain the initial densification of snow
after snowfall.

650

Acknowledgements. This work was funded by the Swiss National Science Foundation (SNSF) through Grant No. 200021 132549.

References

- Arnaud, L., ~~and~~ Picard, G., ~~Champollion, N., Domin, F., Gallet, J. C., Lefebvre, E., Fily, M. and Barnola,~~
655 ~~J. M.~~: Measurement of vertical profiles of snow specific surface area with a 1 cm resolution using infrared
reflectance: instrument description and validation, *J. Glaciol.*, 57, 17–29, 2011.
- Arnaud, L., Barnola, J. M., and Duval, P.: Physical modeling of the densification of snow / firn and ice ~~in the~~
upper part of polar ice sheets, in: *Physics of Ice Core Records*, edited by Hondoh, T., vol. 159, pp. 285–305,
Hokkaido University Press, Sapporo, Japan, 2000.
- 660 Bader, H.: Theory of densification of dry snow on high polar glaciers, *US Army SIPRE Res. Rep.*, 69, 1960.
- Bartelt, P. and Lehning, M.: A physical SNOWPACK model for the Swiss avalanche warning Part I: numerical
model, *Cold Reg. Sci. Technol.*, 35, 123–145, ~~10.1016/S0165-232X(02)00074-5~~, 2002.
- Cabanes, A., Legagneux, L. ~~and Domin,~~ ~~and Domine,~~ F.: Evolution of the specific surface area and of crystal
morphology of Arctic fresh snow during the ALERT 2000 campaign, *Atmos. Environ.*, ~~36~~, 2767–2777,
665 doi:{10.1016/S1352-2310(02)00111-5}, ~~2002~~-2002.
- Cabanes, A., Legagneux, L. ~~and Domin,~~ ~~and Domine,~~ F.: Rate of evolution of the specific surface area of surface
snow layers, *Environ. Sci. Technol.*, ~~37~~, 661–666, ~~10.1021/es025880r~~, ~~2003~~, doi:{10.1021/es025880r},
~~2003~~.
- Calonne, N., Flin, F., Geindreau, C., Lesaffre, B. ~~and du Roscoat,~~ ~~and Rolland du Roscoat,~~ S. R.: Study of a
670 temperature gradient metamorphism of snow from 3-D images: time evolution of microstructures, physical
properties and their associated anisotropy, *Cryosphere Discuss.*, 8, 1407–1451, ~~10.5194/tcd-8-1407-2014~~ doi:
10.5194/tcd-8-1407-2014, <http://www.the-cryosphere-discuss.net/8/1407/2014/>, 2014.
- Carmagnola, C. M., Morin, S., Lafaysse, M., ~~Domin~~Domine, F., Lesaffre, B., Lejeune, Y., Picard, G., and Ar-
naud, L.: Implementation and evaluation of prognostic representations of the optical diameter of snow in the
675 ~~detailed snowpack model~~-SURFEX/ISBA-Crocus ~~detailed snowpack model~~, *The Cryosphere*, ~~Cryosphere~~
~~Discuss.~~, 7, 4443–4500, 2013-8, 417–437, doi:10.5194/tc-8-417-2014, <http://www.the-cryosphere.net/8/417/2014/>, 2014.
- Delmas, L.: Influence of snow type and temperature on snow viscosity, *J. Glaciol.*, 59, 87–92,
~~10.3189/2013JG11J231~~, 2013.
- 680 Dominé, F., Taillandier, A. S. S., and Simpson, W. R.: A parameterization of the specific surface area of
seasonal snow for field use and for models of snowpack evolution, *J. Geophys. Res.*, 112, ~~F02031~~,
~~10.1029/2006jg000512~~, 2007.
- Flanner, M. G. and Zender, C. S.: Linking snowpack microphysics and albedo evolution, *J. Geophys. Res.*, 111,
~~D12208~~, ~~10.1029/2005jd006834~~, 2006.
- 685 Gallet, J.-C., ~~Domin~~Domine, F., Zender, C. S., and Picard, G.: Measurement of the specific surface area of snow
using infrared reflectance in an integrating sphere at 1310 and 1550 nm, *The Cryosphere*, 3, ~~167–182~~167–182,
doi:10.5194/tc-3-167-2009, <http://www.the-cryosphere.net/3/167/2009/>, 2009.
- Jordan, R.: A one-dimensional temperature model for a snow cover: Technical documentation for
SNTHERM.89, CRREL Spec. Rep., 91-16, 1991.
- 690 Kaempfer, T. and Schneebeli, M.: Observation of isothermal metamorphism of new snow and interpretation as
a sintering process, *J. Geophys. Res.*, 112, ~~D24101~~, ~~10.1029/2007JD009047~~, 2007.
- ~~Kerbrat, M., Pinzer, B., Huthwelker, T., Gaeggeler, H., Ammann, M., and Schneebeli, M.: Measuring the~~

- [specific surface area of snow with X-ray tomography and gas adsorption: comparison and implications for surface smoothness, *Atmos. Chem. Phys.*, 8, 1261–1275, 2008.](#)
- 695 Kikuchi, K., Kameda, T., Higuchi, K., and Yamashita, A.: A global classification of snow crystals, ice crystals, and solid precipitation based on observations from middle latitudes to polar regions, *Atmos. Res.*, 132–133, 460–472, 2013.
- Kirchner, H. O. K., Michot, G., Narita, H., and Suzuki, T.: Snow as a foam of ice: plasticity, fracture and the brittle-to-ductile transition, *Philos. Mag. A*, 81, 2161–2181, 2001.
- 700 Kwon, Y., Thornton, K., and Voorhees, P.: Coarsening of bicontinuous structures via nonconserved and conserved dynamics, *Phys. Rev. E*, 75, ~~021120~~, [10.1103/PhysRevE.75.021120](#), 2007.
- [Legagneux, L.: Grain growth theories and the isothermal evolution of the specific surface area of snow, *J. Appl. Phys.*, 95, 6175, 2004.](#)
- Legagneux, L., Cabanes, A., and ~~Domin~~[Domine](#), F.: Measurement of the specific surface area of 176 snow samples using methane adsorption at 77 K, *J. Geophys. Res.*, 107, ~~4335~~, [10.1029/2001jd001016](#), 15, 2002.
- Legagneux, L., Lauzier, T., ~~Domin~~[Domine](#), F., Kuhs, W. F., Heinrichs, T., and Techmer, K.: Rate of decay of specific surface area of snow during isothermal experiments and morphological changes studied by scanning electron microscopy, *Can. J. Phys.*, 81, ~~459–468~~, [10.1139/p03-025-459-468](#), doi:10.1139/P03-025, 2003.
- ~~Legagneux, L., Taillandier, A. S., and Domin, F.: Grain growth theories and the isothermal evolution of the specific surface area of snow, *J. Appl. Phys.*, 95, 6175–6184, 10.1063/1.1710718, 2004.~~
- 710 ~~Legagneux, L. and Domin, F.: A mean field model of the decrease of the specific surface area of dry snow during isothermal metamorphism, *J. Geophys. Res.*, 110, F04011, 10.1029/2004jf000181, 2005.~~
- Lehning, M., Bartelt, P., Brown, B., Fierz, C., and Satyawali, P.: A physical SNOWPACK model for the Swiss avalanche warning Part II. Snow microstructure, *Cold Reg. Sci. Technol.*, 35, 147–167, ~~10.1016/S0165-232X(02)00072-1~~, 2002.
- [Libois, Q., Picard, G., France, J. L., Arnaud, L., Dumont, M., Carmagnola, C. M., and King, M. D.: Influence of grain shape on light penetration in snow, *The Cryosphere*, 7, 1803–1818, doi:10.5194/tc-7-1803-2013, <http://www.the-cryosphere.net/7/1803/2013/>, 2013.](#)
- Löwe, H., Spiegel, J., and Schneebeli, M.: Interfacial and structural relaxations of snow under isothermal conditions, *J. Glaciol.*, 57, 499–510, ~~10.3189/002214311796905569~~, 2011.
- 720 Löwe, H., Riche, F., and Schneebeli, M.: A general treatment of snow microstructure exemplified by an improved relation for thermal conductivity, *Cryosphere*, 7, 1473–1480, ~~10.5194/tc-7-1473-2013~~, 2013.
- Matzl, M. and Schneebeli, M.: Measuring specific surface area of snow by near-infrared photography, *J. Glaciol.*, 52, 558–564, 2006.
- 725 McCreight, J. L. and Small, E. E.: Modeling bulk density and snow water equivalent using daily snow depth observations., *Cryosphere Discuss.*, 7, 5007–5049, ~~10.5194/tcd-7-5007-2013~~, 2013.
- Michelsen, K., DeRaedt, H., and DeHosson, J.: Aspects of mathematical morphology, *Adv. Imag. Elect. Phys.*, 125, 119–194, 2003.
- Perovich, D. K.: Light reflection and transmission by a temperate snow cover, *J. Glaciol.*, 53, 201–210, 2007.
- 730 Petrenko, V. F. and Whitworth, R. W.: *Physics of ice*, Oxford University Press, ~~Oxford~~[USA](#), 1999.
- [Pinzer, B. R. and Schneebeli, M.: Snow metamorphism under alternating temperature gradients: Morphology and recrystallization in surface snow, *Geophys. Res. Lett.*, 36, L23 503, doi:10.1029/2009GL039618, 2009.](#)

- Schleef, S. and Löwe, H.: X-ray microtomography analysis of isothermal densification of new snow under external mechanical stress, *J. Glaciol.*, 59, 233–243, ~~10.3189/2013JG12J076~~, 2013.
- 735 Schleef, S., Jaggi, M., Löwe, H., and Schneebeli, M.: An improved machine to produce nature-identical snow in the laboratory, *J. Glaciol.*, 60, 94–102, ~~10.3189/2014JG13J118~~, 2014a.
- Schleef, S., Löwe, H., and Schneebeli, M.: Hot pressure sintering of ~~low density~~ low density snow analyzed by X-ray microtomography and in-situ ~~microcompression~~ micro-compression, *Acta Mater.*, ~~in press~~ 71, 185–194, 2014b.
- 740 Steinkogler, W., Fierz, C., Lehning, M., and Oblitner, F.: Systematic Assessment of New Snow Settlement in SNOWPACK, in: *International Snow Science Workshop, Davos, Switzerland*, edited by Schweizer, J and VanHerwijnen, A, pp. 132–135, 2009.
- Taillandier, A. ~~S.S.~~, Dominé, F., Simpson, W. ~~R.~~, Sturm, M., and Douglas, T. ~~A.~~ a.: Rate of decrease of the specific surface area of dry snow: Isothermal and temperature gradient conditions, *J. Geophys. Res.*, 112, ~~F03003~~, ~~10.1029/2006JF000514~~, 2007.
- 745 Thompson, G., Field, P. R., Rasmussen, R. M., and Hall, W. D.: Explicit Forecasts of Winter Precipitation Using an Improved Bulk Microphysics Scheme. Part II: Implementation of a New Snow Parameterization, *Mon. Weather Rev.*, 136, 5095–5115, 2008.
- Vetter, R., Sigg, S., Singer, H. M., Kadau, D., Herrmann, H. J., and Schneebeli, M.: Simulating isothermal aging of snow, *Europhys. Lett.*, 89, ~~26001~~, ~~10.1209/0295-5075/89/26001~~ 26 001, 2010.
- 750 Vionnet, V., Brun, E., Morin, S., Boone, ~~Aa.~~, Faroux, S., Le Moigne, P., Martin, E., and Willemet, J.-M.: The detailed snowpack scheme Crocus and its implementation in SURFEX v7.2, *Geosci. Model Develop.*, 5, 773–791, 2012.
- Wiesmann, A., Mätzler, C., and Weise, T.: Radiometric and structural measurements of snow samples, *Radio Science*, 33, 273–289, 1998.
- 755

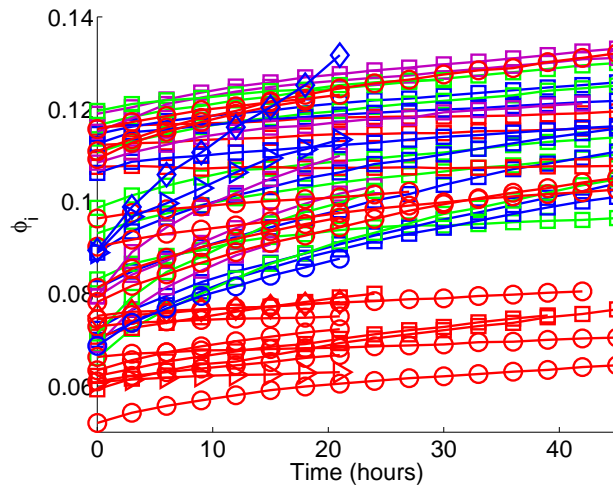


Fig. 1. Evolution of the ice volume fraction ϕ_{ice} for all samples. The color of the symbols (Colors indicate different stress values (red 0 Pa, blue 133 Pa, green 215 Pa, magenta 318 Pa) and the temperature is encoded by Symbols indicated different temperatures: \square -18°C, \circ -13°C, \triangleright -8°C, \diamond -3°C)

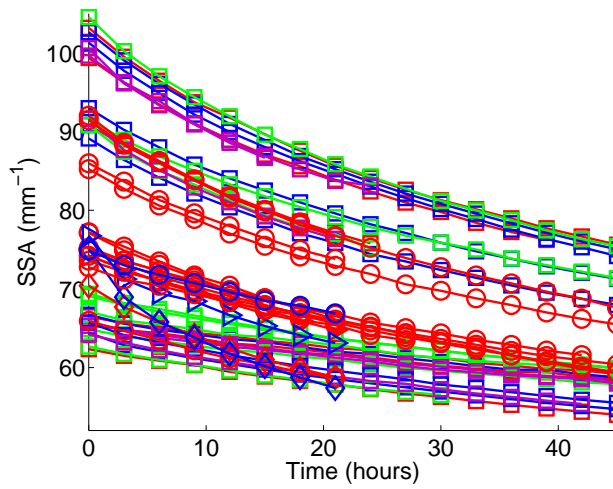


Fig. 2. Evolution of the SSA for all samples. The color of the symbols (Colors indicate different stress values (red 0 Pa, blue 133 Pa, green 215 Pa, magenta 318 Pa) and the temperature is encoded by Symbols indicated different temperatures: \square -18°C, \circ -13°C, \triangleright -8°C, \diamond -3°C)

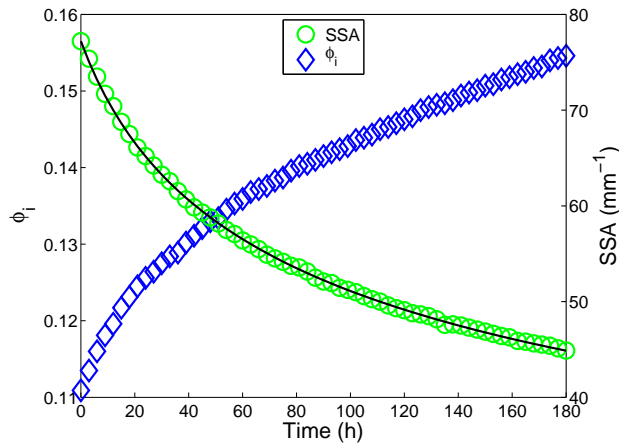


Fig. 3. Evolution of ice volume fraction and SSA in one week at about -13°C . The initial 3d structure and crystal habit of this natural snow sample experiment are shown in Figure 8 (bottom) and listed as snow 5 in Table 1. A fit for the SSA according to Eq. (1) is plotted as black line.

~~Examples of the evolution of the Euler characteristic χ for different new snow types (cf. Table 1) during the first day of settlement. The sample of the week measurement (snow 5, Fig. 3), two examples of snow 9 with different applied stresses belonging to the experiments presented by , and two examples of snow 14 with different applied stresses at -3°C , are shown.~~

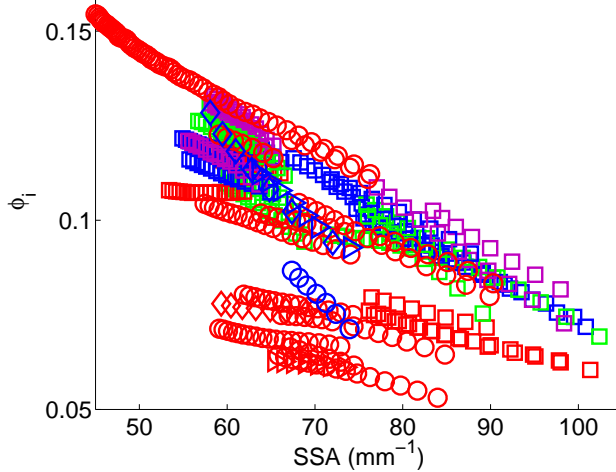


Fig. 4. Comparison between the evolution Plot of the ice volume fraction and versus the specific surface area of our complete data showing SSA for all experiments reveals an almost linear relation for each time series of measurement. Legend: stress indicated by colors: red 0 Pa, blue 133 Pa, green 215 Pa, magenta 318 Pa; temperature indicated by symbols: \square -18°C , \circ -13°C , \triangleright -8°C , \diamond -3°C ; snow types are indistinguishable.

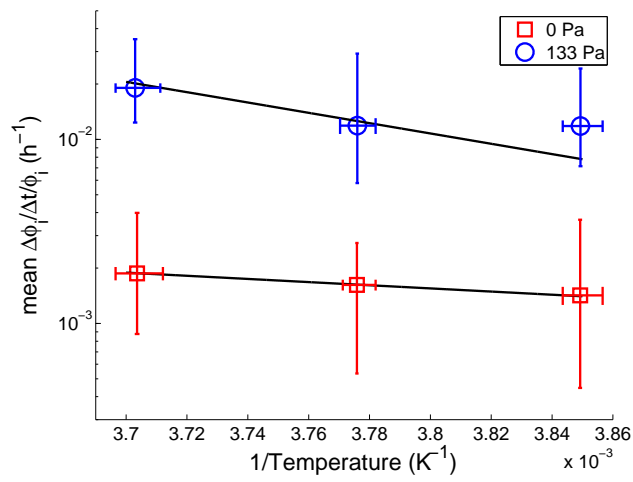


Fig. 5. Mean densification rate for experiments at different temperatures averaged over 24h as a function of temperature.

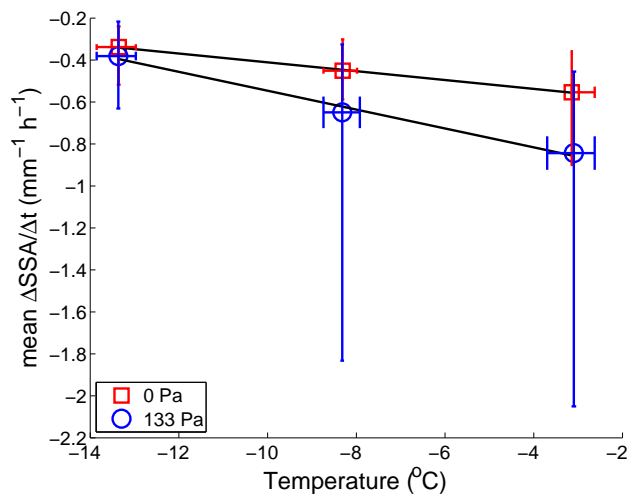


Fig. 6. Mean-SSA decay rate averaged over 24h as a function of temperature.

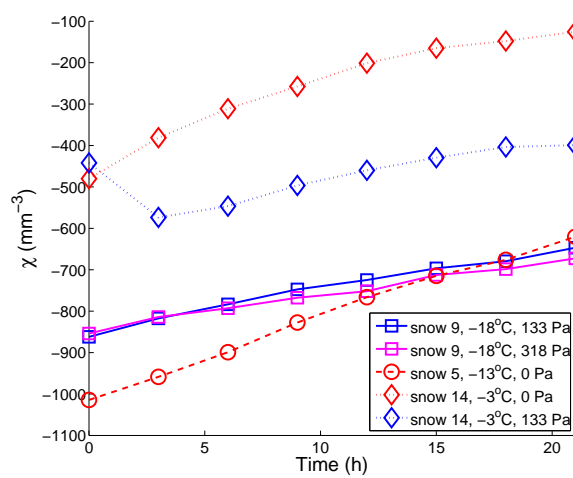


Fig. 7. Selected examples of the evolution of the Euler characteristic χ for ~~experiments at~~ different ~~temperatures~~ new snow types (cf. Table 1) during the first day of settlement: The one-week measurement (snow 5, Fig. 3), two examples of snow 9 with different applied stresses (taken from Schleef and Löwe (2013)), and two examples of snow 14 with different, applied stresses at -3°C.

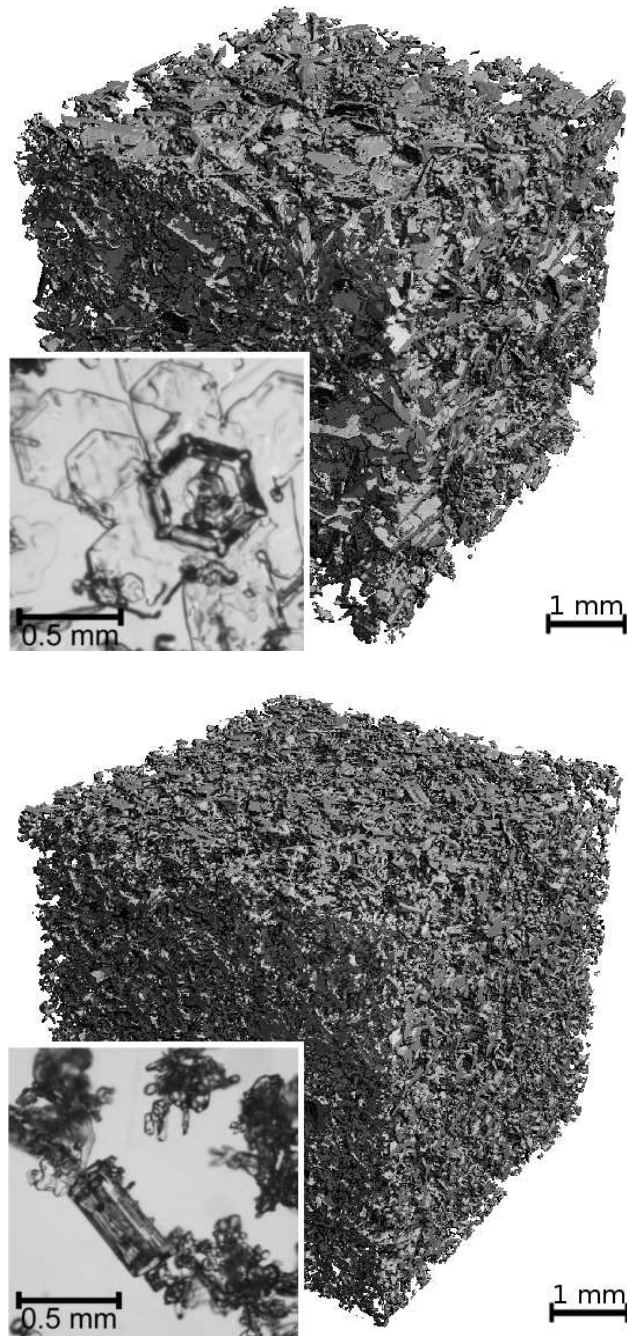


Fig. 8. Examples of natural snow samples with a photograph of the **exemplary** crystal habit and an μ CT image of the initial structure. The parameters of the sample at top are $\phi_{ice,0} \approx 0.1$, $\phi_{i,0} \approx 0.1$ and $SSA_0 \approx 62 \text{mm}^{-1}$ (snow 2 in Table 1), and of the sample at bottom $\phi_{ice,0} \approx 0.1$, $\phi_{i,0} \approx 0.1$ and $SSA_0 \approx 77 \text{mm}^{-1}$ (snow 5 in Table 1, evolution shown in Fig. 3).

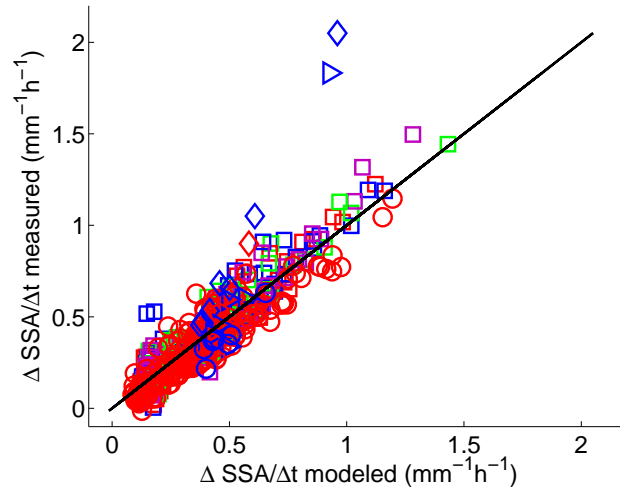


Fig. 9. Modeled Scatter plot of SSA change according to decay rates SSA, computed from Eq. (4) (horizontal axis) versus measuring results measurements. Legend: stress Different stresses are indicated by colors: red 0 Pa, blue 133 Pa, green 215 Pa, magenta 318 Pa; temperature different temperatures are indicated by the symbols: \square -18°C, \circ -13°C, \triangleright -8°C, \diamond -3°C; snow types are indistinguishable.

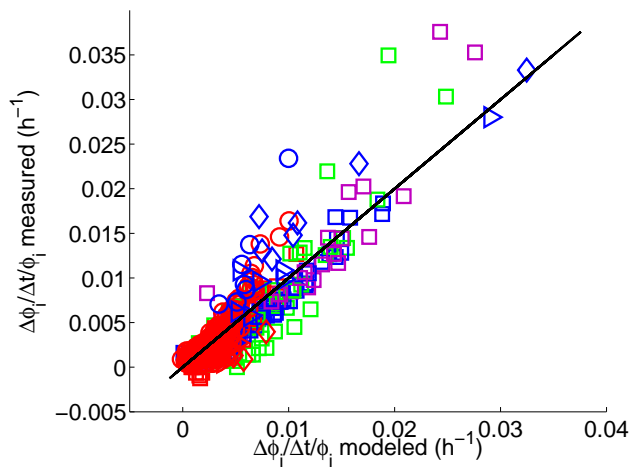


Fig. 10. Modeled Scatter plot of densification rates $\dot{\phi}/\phi$ according to, computed from Eq. (7) (horizontal axis) versus measuring results measurements (vertical axis). Legend: stress Different stresses are indicated by colors: red 0 Pa, blue 133 Pa, green 215 Pa, magenta 318 Pa; temperature different temperatures are indicated by symbols: \square -18°C, \circ -13°C, \triangleright -8°C, \diamond -3°C; snow types are indistinguishable.

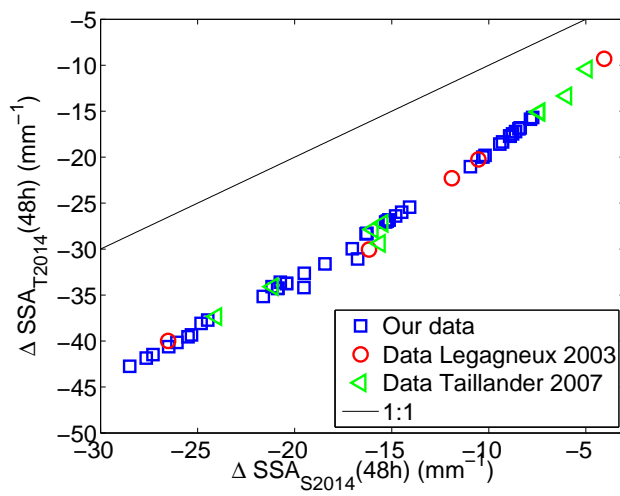


Fig. 11. Scatter plot of the predicted SSA difference $\Delta\text{SSA}(48\text{h})$ after 48h, obtained from the parametrizations Eq. (13) in Taillander et al. (2007) (vertical axis) and from the present parametrization, Eq. (5) (horizontal axis), which were respectively applied to the different available datasets (legend). See text for further details.

Table 1. Overview of experiments. Set IDs (1-8) correspond to natural snow while (9-14) are ~~nature-identical snowmaker~~ snow ~~samples grown in the lab~~. The sets 9 and 10 were already used in Schleef and Löwe (2013) and included here for comparison. For each set the number of samples N_s and the total number of measurements N_m ~~from the~~ ~~per sample in a~~ time series are given in addition to applied stresses σ and used temperatures T . The initial values of ice fraction $\bar{\phi}_{ice,0}$ and specific surface area \overline{SSA}_0 are averages over all samples within the set. For all observed crystal habits the classification number is given according to Kikuchi et al. (2013), including potentially broken parts (I3a) of them.

Snow ID	N_s	N_m	σ Pa	T °C	$\bar{\phi}_{ice,0}$	\overline{SSA}_0 mm ⁻¹	Class. No.
1	2	32	133, 215	-18	0.08	92	P3a, P3b, R1c, H1a, I2a
2	5	76	0, 133, 215, 318	-18	0.11	64	P2b, P4c, P4d
3	7	90	0, 133, 215, 318	-18	0.07	102	P3a, R1c, I2a
4	4	43	0, 133, 215, 318	-18	0.08	91	P3b, R1c
5	2	68	0	-13	0.11	77	C3b, C3c, C4d, P3a, P3b, A1a
6	2	30	0	-13	0.09	75	P3b, P4e, P4f, A2a, R1c
7	2	24	0	-13	0.08	92	C4b, C4d, P2b, H1a, H1b
8	2	24	0	-13	0.06	86	P1a, P2a, P3a, P3b, P4e, P4g
9	7	111	0, 133, 215, 318	-18	0.11	66	not analyzed
10	2	32	215	-18	0.10	69	not analyzed
11	1	19	0	-13	0.07	74	P3b, P3c, P4c
12	2	23	0	-13	0.07	75	P3b, P3c
13	1	8	0	-13	0.12	66	C1a, C1b, C1c, I1a
14	6	48	0, 133	-3, -8, -13	0.08	74	P3b, P3c